

# Decoupling and antiresonance in electronic transport through a quantum dot chain embodied in an Aharonov-Bohm interferometer

Yu Han<sup>a,b</sup>, Weijiang Gong<sup>a,\*</sup>, Haina Wu<sup>a</sup>, and Guozhu Wei<sup>a,c</sup>

*a. College of Sciences, Northeastern University, Shenyang 110004, China*

*b. Department of Physics, Liaoning University, Shenyang 110036, China*

*c. International Center for Material Physics, Academia Sinica, Shenyang 110015, China*

(Dated: February 13, 2009)

**Abstract** Electronic transport through a quantum dot chain embodied in an Aharonov-Bohm interferometer is theoretically investigated. In such a system, it is found that only for the configurations with the same-numbered quantum dots side-coupled to the quantum dots in the arms of the interferometer, some molecular states of the quantum dot chain decouple from the leads. Namely, in the absence of magnetic flux all odd molecular states decouple from the leads, but all even molecular states decouple from the leads when an appropriate magnetic flux is introduced. Interestingly, the antiresonance position in the electron transport spectrum is independent of the change of the decoupled molecular states. In addition, when considering the many-body effect within the second-order approximation, we show that the emergence of decoupling gives rise to the apparent destruction of electron-hole symmetry. By adjusting the magnetic flux through either subring, some molecular states decouple from one lead but still couple to the other, and then some new antiresonances occur.

PACS numbers: 73.63.Kv, 73.21.La, 73.21.Hk, 85.38.Be

Keywords: Quantum dot; Decoupling; Antiresonance

## I. INTRODUCTION

During the past years, electronic transport through quantum-dot(QD) systems has been extensively studied both experimentally and theoretically. The atom-like characteristics of a QD, such as the discrete electron levels and strong electron correlation, manifest themselves by the experimental observations of Coulomb blockade[1, 2, 3, 4], conductance oscillation[5], and Kondo effect[6, 7, 8, 9] in electronic transport through a QD. Therefore, a single QD is usually called an artificial atom, and a mutually coupled multi-QD system can be regarded as an artificial molecule. Thanks to the progress of nanotechnology, it now becomes possible to fabricate a variety of coupled QD structures with sizes to be smaller than the electron coherence[10, 11]. In comparison with a single QD, coupled QD systems possess higher freedom in implementing some functions of quantum devices, such as the QD cellular automata[12] and solid-state quantum computation[13, 14].

Motivated by an attempt to find some interesting electron transport properties, recently many experimental and theoretical works have become increasingly concerned about the electronic transport through various multi-QD systems[15, 16, 17, 18, 19]. According to the previous researches, the peaks of the linear conductance spectra of coupled-QD systems reflect the eigenenergies of the corresponding coupled QDs. On the contrary, the zero point of the conductance, called antiresonance, originates from

the destructive quantum interference among electron waves passing through different transmission paths. With respect to the coupled-QD structures, the typical ones are the structures of the so-called T-shaped QDs [20, 21, 22, 23, 24, 25] and the parallel QDs [26, 27, 28, 29] (i.e., the QDs embodied in the Aharonov-Bohm (AB) interferometer). A unique property of electron transport through the T-shaped QD systems is that the antiresonance points coincide with the eigenenergies of the side-coupled QDs, which has also been observed experimentally[20, 21]. On the other hand, the parallel-coupled QD systems, which offer two channels for the electron tunneling, have also attracted much attention. In such structures, with the adjustment of magnetic flux the AB effect has been observed. Meanwhile, the appropriate couplings between the molecular states of the coupled QDs and leads can be efficiently adjusted, which gives rise to the tunable Fano effect[27, 28]. Moreover, under the condition of an appropriate external field, some molecular states can decouple completely from the leads, which is referred to as the formation of bound states in continuum in some literature[30]. According to the previous researches, the existence of decoupling plays a non-trivial role in the quantum interference of QD structures, especially, it changes the property of the quantum interference[31]. Therefore, it is still desirable to clarify the decoupling in electronic transport through some coupled-QD structures.

Since the development of nanotechnology, it is feasible to fabricate the coupled QDs, in particular the QD chain, in the current experiment[32, 33]. Thereby we are now theoretically concerned with the electron transport properties of the this structure, by considering it embodied in the AB interferometer. As a result, we find that for the structures with the same-numbered QDs side-coupled to the QDs in

---

\*Corresponding author. Fax: +086-024-8367-6883; phone: +086-024-8367-8327; Email address: weijianggong@gmail.com

the two arms of the interferometer, some molecular states of the QD chain decouple from the leads, and which molecular states decouple from the leads is determined by the adjustment of magnetic flux. Besides, in the case of the many-body effect being considered, the existence of decoupling gives rise to the destruction of electron-hole symmetry.

## II. MODEL

The coupled-QD structure we consider is illustrated in Fig.1(a). The Hamiltonian that describes the electronic motion in such a structure reads  $H = H_C + H_D + H_T$ , in which  $H_C$  is the Hamiltonian for the noninteracting electrons in the two leads,  $H_D$  describes the electron in the QD chain, and  $H_T$  denotes the electron tunneling between the leads and QDs. They take the forms as follows.

$$\begin{aligned}
H_C &= \sum_{\sigma k \alpha \in L, R} \varepsilon_{k\alpha} c_{k\alpha\sigma}^\dagger c_{k\alpha\sigma}, \\
H_D &= \sum_{\sigma, m=1}^N \varepsilon_m d_{m\sigma}^\dagger d_{m\sigma} + \sum_m U_m n_{m\uparrow} n_{m\downarrow} \\
&\quad + \sum_{\sigma, m=1}^{N-1} (t_m d_{m+1\sigma}^\dagger d_{m\sigma} + \text{H.c.}), \\
H_T &= \sum_{k\alpha\sigma} (V_{\alpha j} d_{j\sigma}^\dagger c_{k\alpha\sigma} + V_{\alpha j+1} d_{j+1\sigma}^\dagger c_{k\alpha\sigma} + \text{H.c.}),
\end{aligned} \tag{1}$$

where  $c_{k\alpha\sigma}^\dagger$  ( $c_{k\alpha\sigma}$ ) is an operator to create (annihilate) an electron of the continuous state  $|k, \sigma\rangle$  in lead- $\alpha$  with  $\sigma$  being the spin index, and  $\varepsilon_{k\alpha}$  is the corresponding single-particle energy.  $d_{m\sigma}^\dagger$  ( $d_{m\sigma}$ ) is the creation (annihilation) operator of electron in QD- $m$ ,  $\varepsilon_m$  denotes the electron level in the corresponding QD,  $t_m$  is the interdot hopping coefficient, and  $U_m$  represents the intradot Coulomb repulsion.  $n_{m\sigma} = d_{m\sigma}^\dagger d_{m\sigma}$  is the electron number operator in QD- $m$ . We assume that only one level is relevant in each QD and the value of  $\varepsilon_m$  is independent of  $m$ , i.e.,  $\varepsilon_m = \varepsilon_0$ . In the expression of  $H_T$ , the sequence numbers of the two QDs in the interferometer arms are taken as  $j$  and  $j+1$ , and  $V_{\alpha j}$  and  $V_{\alpha j+1}$  with  $\alpha = L, R$  denotes the QD-lead coupling coefficients. We adopt a symmetric QD-lead coupling configuration which gives that  $V_{Lj} = V e^{i\phi_L/2}$ ,  $V_{Lj+1} = V e^{-i\phi_L/2}$ ,  $V_{Rj} = V e^{-i\phi_R/2}$ , and  $V_{Rj+1} = V e^{i\phi_R/2}$  with  $V$  being the QD-lead coupling strength. The phase shift  $\phi_\alpha$  is associated with the magnetic flux  $\Phi_\alpha$  threading the system by a relation  $\phi_\alpha = 2\pi\Phi_\alpha/\Phi_0$ , in which  $\Phi_0 = h/e$  is the flux quantum.

To study the electronic transport properties of such a structure, the linear conductance at zero temperature is obtained by the Landauer-Büttiker formula

$$\mathcal{G} = \frac{e^2}{h} \sum_{\sigma} T_{\sigma}(\omega)|_{\omega=\varepsilon_F}. \tag{2}$$

$T(\omega)$  is the transmission function, in terms of Green function which takes the form as [34, 35]

$$T_{\sigma}(\omega) = \text{Tr}[\Gamma^L G_{\sigma}^r(\omega) \Gamma^R G_{\sigma}^a(\omega)], \tag{3}$$

where  $\Gamma^L$  is a  $2 \times 2$  matrix, describing the strength of the coupling between lead-L and the QDs in the interferometer arms. It is defined as  $[\Gamma^L]_{ll'} = 2\pi V_{Ll} V_{Ll'}^* \rho_L(\omega)$  ( $l, l' = [j, j+1]$ ). We will ignore the  $\omega$ -dependence of  $\Gamma_{ll'}^L$  since the electron density of states in lead-L,  $\rho_L(\omega)$ , can be usually viewed as a constant. By the same token, we can define  $[\Gamma^R]_{ll'}$ . In fact, one can readily show that  $[\Gamma^L]_{ll} = [\Gamma^R]_{ll}$  in the case of identical QD-lead coupling, hence we take  $\Gamma = [\Gamma^L]_{ll} = [\Gamma^R]_{ll}$  to denote the QD-lead coupling function. In Eq. (3) the retarded and advanced Green functions in Fourier space are involved. They are defined as follows:  $G_{ll',\sigma}^r(t) = -i\theta(t)\langle\{d_{l\sigma}(t), d_{l'\sigma}^\dagger\}\rangle$  and  $G_{ll',\sigma}^a(t) = i\theta(-t)\langle\{d_{l\sigma}(t), d_{l'\sigma}^\dagger\}\rangle$ , where  $\theta(x)$  is the step function. The Fourier transforms of the Green functions can be performed via  $G_{ll',\sigma}^{r(a)}(\omega) = \int_{-\infty}^{\infty} G_{ll',\sigma}^{r(a)}(t) e^{i\omega t} dt$ . These Green functions can be solved by means of the equation-of-motion method [36, 37]. By a straightforward derivation, we obtain the retarded Green functions which are written in a matrix form as

$$G_{\sigma}^r(\omega) = \begin{bmatrix} g_{j\sigma}(z)^{-1} & -t_j + i\Gamma_{j,j+1} \\ -t_j^* + i\Gamma_{j+1,j} & g_{j+1\sigma}(z)^{-1} \end{bmatrix}^{-1}, \tag{4}$$

with  $z = \omega + i0^+$  and  $\Gamma_{ll'} = \frac{1}{2}([\Gamma^L]_{ll'} + [\Gamma^R]_{ll'})$ .  $g_{l\sigma}(z) = [(z - \varepsilon_l)S_{l\sigma} - \Sigma_{l\sigma} + i\Gamma_{ll}]^{-1}$ , is the zero-order Green function of the QD- $l$  unperturbed by QD- $l'$ , in which the selfenergies

$$\begin{aligned}
\Sigma_{j\sigma} &= \frac{t_{j-1}^2}{(z - \varepsilon_{j-1})S_{j-1\sigma} - \frac{t_{j-2}^2}{(z - \varepsilon_{j-2})S_{j-2\sigma} - \dots - \frac{t_1^2}{(z - \varepsilon_2)S_{2\sigma} - \frac{t_1^2}{(z - \varepsilon_1)S_{1\sigma}}}} \\
\Sigma_{j+1\sigma} &= \frac{t_{j+1}^2}{(z - \varepsilon_{j+1})S_{j+1\sigma} - \frac{t_{j+2}^2}{(z - \varepsilon_{j+2})S_{j+2\sigma} - \dots - \frac{t_{N-1}^2}{(z - \varepsilon_{N-1})S_{N-1\sigma} - \frac{t}{(z - \varepsilon_N)S_{N\sigma}}}}
\end{aligned}$$

account for the laterally coupling of the QDs to QD- $j$  and QD- $j+1$ , respectively [36]. The quantity  $S_{m\sigma} = \frac{z - \varepsilon_m - U_m}{z - \varepsilon_m - U_m + U_m \langle n_{m\sigma} \rangle}$  ( $m \in [1, N]$ ) is the contribution of the intradot Coulomb interaction up to the second-order approximation [25]. In addition, the advanced Green function can be readily obtained via a relation  $G_{\sigma}^a(\omega) = [G_{\sigma}^r(\omega)]^\dagger$ .

It is easy to understand that in the noninteracting case, the linear conductance spectrum of the coupled QD structure reflects the eigenenergy spectrum of the “molecule” made up of the coupled QDs. In other words, each resonant peak in the conductance spectrum represents an eigenenergy of the total QD molecule, rather than the levels of the individual

QDs. Therefore, it is necessary to transform the Hamiltonian into the molecular orbital representation of the QD chain. We now introduce the electron creation(annihilation) operators corresponding to the molecular orbits, i.e.,  $f_{m\sigma}^\dagger$  ( $f_{m\sigma}$ ). By the diagonalization of the single-particle Hamiltonian of the QDs, we find the relation between the molecular and atomic representations (here each QD is regarded as an ‘‘atom’’). It is expressed as  $[f_{\sigma}^\dagger] = [\eta][d_{\sigma}^\dagger]$ . The  $N \times N$  transfer matrix  $[\eta]$  consists of the eigenvectors of the QD Hamiltonian. In the molecular orbital representation, the single-particle Hamiltonian takes the form:  $H = \sum_{k\sigma\alpha \in L,R} \varepsilon_{\alpha k} c_{\alpha k\sigma}^\dagger c_{\alpha k\sigma} + \sum_{m=1,\sigma} e_m f_{m\sigma}^\dagger f_{m\sigma} + \sum_{\alpha k\sigma} v_{\alpha m} f_{m\sigma}^\dagger c_{\alpha k\sigma} + \text{h.c.}$ , in which  $e_m$  is the eigenenergy of the coupled QDs. The coupling between the molecular state  $|m\sigma\rangle$  and the state  $|k, \sigma\rangle$  in lead- $\alpha$  can be expressed as

$$v_{\alpha m} = V_{\alpha j} [\eta]_{jm}^\dagger + V_{\alpha j+1} [\eta]_{j+1,m}^\dagger. \quad (5)$$

In the case of symmetric QD-lead coupling, the above relation can be rewritten as  $v_{\alpha m} = V([\eta]_{jm}^\dagger + [\eta]_{j+1,m}^\dagger e^{i\phi_\alpha})$ . Fig.1(b) shows the illustration of the QD structure in the molecular orbital representation. We here define  $\gamma_{mm}^\alpha = 2\pi v_{\alpha m} v_{\alpha m}^* \rho_\alpha(\omega)$  which denotes the strength of the coupling between the molecular state  $|m\sigma\rangle$  and the leads.

### III. NUMERICAL RESULTS AND DISCUSSIONS

With the theory in the above section, we can perform the numerical calculation to investigate the linear conductance spectrum of this variational parallel double-QD structures, namely, to calculate the conductance as a function of the incident electron energy. Prior to the calculation, we need to introduce a parameter  $t_0$  as the unit of energy.

We choose the parameter values  $t_m = \Gamma = t_0$  for the QDs to carry out the numerical calculation. And  $\varepsilon_0$ , the QD level, can be shifted with respect to the Fermi level by the adjustment of gate voltage experimentally. Typically, the case of  $\phi_L = \phi_R = \phi$  are first considered. Fig.2 shows the linear conductance spectra ( $\mathcal{G}$  versus  $\varepsilon_0$ ) for several structures with the QD number  $N = 2$  to 4. It is obvious that the 2-QD structure just corresponds to the parallel double QDs with interdot coupling mentioned in some previous works[27, 28]. Its conductance spectrum presents a Breit-Wigner lineshape in the absence of magnetic flux, as shown in Fig.2(a). Such a result can be analyzed in the molecular orbital representation. Here the  $[\eta]$  matrix, takes a form as  $[\eta] = \frac{1}{\sqrt{2}} \begin{bmatrix} -1 & 1 \\ 1 & 1 \end{bmatrix}$ , presenting the relation between the molecular and ‘atomic’ representations. Then with the help of Eq. (5) one can find that here the bonding state completely decouples from

the leads and only the antibonding state couples to the leads, which leads to the appearance of the Breit-Wigner lineshape in the conductance spectrum. On the other hand, when introducing the magnetic flux with  $\phi = \pi$ , we can see that the decoupled molecular state is changed as the antibonding state, as exhibited by the dashed line in Fig.2(a). In such a case, only the bonding state couples to the leads and the conductance profile also shows a Breit-Wigner lineshape.

In Fig.2(b) the conductance curves as a function of gate voltage are shown for the 3-QD structure. Obviously, there exist three conductance peaks in the conductance profiles and no decoupled molecular state appears. We can clarify this result by calculating  $v_{\alpha m} = V([\eta]_{jm}^\dagger + [\eta]_{j+1,m}^\dagger e^{i\phi})$ . Via such a relation, one can conclude that  $v_{\alpha m}$  is impossible to be equal to zero in this structure regardless of the adjustment of magnetic flux. Thus one can not find the decoupled molecular states, the state-lead coupling may be relatively weak, though. Just as shown in Fig.2(b), in the absence of magnetic flux the distinct difference of the couplings between the molecular states and leads offer the ‘more’ and ‘less’ resonant channels for the quantum interference. Then the Fano effect occurs and the conductance profile presents an asymmetric lineshape. In addition, the Fano lineshape in the conductance spectrum is reversed by tuning the magnetic flux to  $\phi = \pi$ , due to the modulation of magnetic flux on  $v_{\alpha m}$ .

When the QD number increases to  $N = 4$ , there will be two configurations corresponding to this structure, i.e, the cases of  $j = 1$  and  $j = 2$ . As a consequence, the conductance spectra of the two structures remarkably differ from each other. With respect to the configuration of  $j = 1$ , as shown in Fig.2(c), the electron transport properties presented by the conductance spectra are similar to those in the case of the 3-QD structure, and there is also no existence of decoupled molecular states. However, for the case of  $j = 2$ , as shown in Fig.2(d), it is clear that in the absence of magnetic flux, there are two conductance peaks in the conductance spectrum, which means that the decoupling phenomenon comes into being. Alternatively, in the case of  $\phi = \pi$ , there also exist two peaks in the conductance profile. But the conductance peaks in the two cases of  $\phi = 0$  and  $\pi$  do not coincide with one another. We can therefore find that in this structure, when  $\phi = n\pi$  the decoupling phenomena will come about, and the adjustment of magnetic flux can effectively change the appearance of decoupled molecular states. By a further calculation and focusing on the conductance spectra, we can understand that in the case of  $\phi = 2n\pi$ , the odd (first and third) molecular states of the coupled QDs decouple from the leads; In contrast, the even (second and fourth) molecular states of the QDs will decouple from the leads if  $\phi = (2n-1)\pi$ . Additionally, in Fig.2(d) it shows that the conductance always encounters its zero when the

level of the QDs is the same as the Fermi level of the system, which is irrelevant to the tuning of magnetic flux from  $\phi = 0$  to  $\pi$ .

In order to obtain a clear physics picture about decoupling, we analyze this problem in the molecular orbital representation. By solving the  $[\eta]$  matrix and borrowing the relation  $v_{\alpha m} = V_{\alpha j}[\eta]_{jm}^\dagger + V_{\alpha j+1}[\eta]_{j+1,m}^\dagger$ , it is easy to find that in the case of zero magnetic flux,  $v_{\alpha 1}$  and  $v_{\alpha 3}$  are always equal to zero, which brings out the completely decoupling of the odd molecular states from the leads. Unlike this case, when  $\phi = \pi$  the values of  $v_{\alpha 2}$  and  $v_{\alpha 4}$  are fixed at zero, and such a result leads to the even molecular states to decouple from the leads. However, the underlying physics responsible for antiresonance is desirable to clarify. We then analyze the electron transmission by the representation transformation. We take the case of  $\phi = 0$  as an example, where only two molecular states  $|2\sigma\rangle$  and  $|4\sigma\rangle$  couple to the leads due to decoupling. Accordingly,  $|2\sigma\rangle$  and  $|4\sigma\rangle$  might be called as well the bonding and antibonding states. As is known, the molecular orbits of coupled double QD structures, e.g, the well-known T-shaped QDs, are regarded as the bonding and antibonding states. Therefore, by employing the representation transformation  $[\alpha_\sigma^\dagger] = [\beta][f_\sigma^\dagger]$ , such a configuration can be changed into the T-shaped double-QD system (see Fig.1(c)) of the Hamiltonian  $\mathcal{H} = \sum_{k\sigma\alpha\in L,R} \varepsilon_{\alpha k} c_{\alpha k\sigma}^\dagger c_{\alpha k\sigma} +$

$$\sum_{\sigma,n=1}^2 E_n a_{n\sigma}^\dagger a_{n\sigma} + \tau_1 a_{2\sigma}^\dagger a_{1\sigma} + \sum_{\alpha k\sigma} w_{\alpha 1} a_{1\sigma}^\dagger c_{\alpha k\sigma} + h.c..$$

By a further derivation, the relations between the structure parameters of the two QD configurations can be obtained with  $E_1 = \varepsilon_0 + t_0$ ,  $E_2 = \varepsilon_0$ ,  $\tau_1 = t_0$ , and  $w_{\alpha 1} = V_{\alpha 1}$  respectively with  $[\beta] = \frac{1}{\sqrt{2\sqrt{5}}} \begin{bmatrix} -\sqrt{\sqrt{5}-1} & \sqrt{\sqrt{5}+1} \\ \sqrt{\sqrt{5}+1} & \sqrt{\sqrt{5}-1} \end{bmatrix}$ . The 4-QD structure is then transformed into the T-shaped double QDs with  $\varepsilon_0$  being the level of dangling QD. Just as discussed in the previous works[25], in the T-shaped QDs antiresonance always occurs when the dangling QD level is aligned with the Fermi level of the system, one can then understand that in this 4-QD system, the antiresonant point in the conductance spectrum is consistent with  $\varepsilon_0 = \varepsilon_F = 0$ . When paying attention to the  $[\eta]^\dagger$  matrix, one will see that  $[\eta]_{12}^\dagger = [\eta]_{43}^\dagger$ ,  $[\eta]_{22}^\dagger = -[\eta]_{33}^\dagger$ ,  $[\eta]_{32}^\dagger = [\eta]_{23}^\dagger$ , and  $[\eta]_{42}^\dagger = -[\eta]_{13}^\dagger$  for the 4-QD structure. As a result, such relations give rise to  $v_{\alpha 2}|_{\phi=0} = v_{\alpha 3}|_{\phi=\pi}$  and  $v_{\alpha 4}|_{\phi=0} = v_{\alpha 1}|_{\phi=\pi}$ . So, when  $\phi = \pi$  the magnetic flux reverses the lineshape of the conductance spectrum in the case of  $\phi = 0$ . Based on these properties, we can realize that the quantum interference in the  $\phi = \pi$  case is similar to that in the case of  $\phi = 0$ . Therefore, the antiresonant point in the conductance spectra is independent of the adjustment of magnetic flux.

Similar to the analysis above, we can expect that

in the structure of with  $t_m = t_0$  and  $\varepsilon_m = \varepsilon_0$ , when  $N$  is even and  $j = \frac{N}{2}$  there must be the appearance of decoupled molecular states. To be concrete, in the case of  $\phi = 2n\pi$ , the odd (first and third) molecular states of the coupled QDs decouple from the leads, whereas the even (second and fourth) molecular states of the QDs will decouple from the leads if  $\phi = (2n-1)\pi$ . This expectation can be confirmed because of  $[\eta]_{jm}^\dagger = -[\eta]_{j+1,m}^\dagger$  ( $m \in \text{odd}$ ) and  $[\eta]_{jm}^\dagger = [\eta]_{j+1,m}^\dagger$  ( $m \in \text{even}$ ) for the QDs. The numerical results in Fig.3, describing the conductances of 6-QD and 8-QD structures, can support our conclusion. Besides, with the help of the representation transformation the antiresonance positions can be clarified by transforming these structure into the T-shaped QD systems.

Fig.4 shows the calculated conductance spectra of the double-QD structure by incorporating the many-body effect to the second order and considering the uniform on-site energies of all the QDs  $U_m = U = 2t_0$  as well as  $4t_0$ , respectively. It is seen that the conductance spectra herein split into two groups due to the Coulomb repulsion. But in each group the present decoupling phenomenon and antiresonance are similar to those in the noninteracting case. In addition, for each case ( $U = 2t_0$  or  $4t_0$ ) between the two separated groups a conductance zero emerges in the conductance spectra. According to the previous discussions, when the many-body terms are considered within the second-order approximation, a pseudo antiresonance, resulting from the electron-hole symmetry, should occur at the position of  $\varepsilon_0 = -\frac{U}{2}$  where  $\langle n_{m\sigma} \rangle = \frac{1}{2}$  [25, 36, 37]. However, with respect to such a situation, unlike the conventional electron-hole symmetry, the position of such a conductance zero departs from  $\varepsilon_0 = -\frac{U}{2}$  remarkably. Taking the structure of double QDs as an example, in the absence of magnetic flux, this conductance zero appears at the position of  $\varepsilon_0 = -\frac{3}{2}t_0$  when  $U = 2t_0$ , but it presents itself at the point of  $\varepsilon_0 = -3t_0$  in the case of  $U = 4t_0$ , as shown in Fig.4(a) and (c). Meanwhile, we can obtain mathematically that around the point of  $\varepsilon_0 = -\frac{U}{2}$ , the average electron occupation number  $\langle n_{m\sigma} \rangle$  is not equal to  $\frac{1}{2}$  any more. Hence, the presence of decoupled molecular state destroys the electron-hole symmetry. All these numerical results can be explained as follows. For such a double-QD structure, one can understand that when the many-body terms are considered within the second-order approximation, the molecular levels are given by  $\varepsilon_0 - t_0, \varepsilon_0 + t_0, \varepsilon_0 - t_0 + U$ , and  $\varepsilon_0 + t_0 + U$ , respectively. So, when  $\varepsilon_0 = -\frac{U}{2}$ , they distribute symmetrically about the Fermi level of the system, which results in  $\langle n_{m\sigma} \rangle = \frac{1}{2}$  and  $\mathcal{G} = 0$ . But, since the unique QD-lead coupling manner of our model, in the absence of magnetic flux the bonding states (with the levels  $\varepsilon_0 - t_0$  and  $\varepsilon_0 - t_0 + U$ ) completely decouple from the leads and only the other two states ( $\varepsilon_0 + t_0$  and  $\varepsilon_0 + t_0 + U$ ) provide the channels for the

electron transport. Obviously, under the condition of  $\varepsilon_0 = -\frac{U}{2}$  the levels  $\varepsilon_0 + t_0$  and  $\varepsilon_0 + t_0 + U$  do not distribute symmetrically about the Fermi level of the system, thus the electron-hole symmetry is broken, which shows itself as the result of  $\langle n_{m\sigma} \rangle \neq \frac{1}{2}$ . Alternatively, in the case of  $\phi = \pi$ , only the bonding states couple to the leads, which also destroys the electron-hole symmetry, corresponding to the results in Fig.4(b) and (d). The case of 4-QD structure, as shown Fig.5, can also be clarified based on such an approach.

Next we turn to focus on the situation of  $\phi_\alpha = n\pi$  and  $\phi_{\alpha'} \neq n\pi$ . By virtue of Eq.(5) we can expect that for such a case, some molecular states of the QDs will decouple from lead- $\alpha$  but they still couple to lead- $\alpha'$ . In Fig. 6 it shows the research on the electron transport within the double-QD and four-QD  $j = 2$  structures. For the double-QD structure, it is obvious that in the case of  $\phi_L = 0$  and  $\phi_R = 0.5\pi$  both the bonding and antibonding states couple to lead-R but the bonding state decouples from lead-L. The corresponding numerical result is shown in Fig.6(a). Clearly, due to the decoupling of the bonding state from lead-L, antiresonance occurs at the position of  $\varepsilon_0 = t_0$ . This means that in this case antiresonance will come about when the level of such a decoupled molecular state is consistent with the Fermi level, corresponding to the discussions in the previous works[37]. In the case of  $\phi_L = 0$  and  $\phi_R = \pi$ , the bonding state decouples from lead-L with the antibonding state decoupled from lead-R. So herein there is no channel for the electron tunneling and the conductance is always equal to zero, despite the shift of QD level, corresponding to the dotted line in Fig.6(a). On the other hand, by fixing  $\phi_R = \pi$  and increasing  $\phi_L$  to  $0.5\pi$ , one will see that the decoupling of antibonding state from lead-R results in the antiresonance at the point of  $\varepsilon_0 = -t_0$ . With regard to the 4-QD  $j = 2$  structure, the decoupling-induced antiresonance is also remarkable in the case of  $\phi_\alpha = n\pi$  and  $\phi_{\alpha'} \neq n\pi$ . As shown in Fig.6(b) there are two kinds of antiresonant points in such a case: One originates from the quantum interference between the coupled molecular states, and the other is caused by the decoupling of some molecular states. With respect to the many-body effect, as shown in Fig. 6(c), apart from the appearance of two groups in the conductance spectra, the electron-hole symmetry remains, which is due to that there is no completely decoupling of the molecular states from the leads in such a case.

In Fig.7 the linear conductances of the semi-infinite and infinite QD chains are presented as a function of gate voltage. As shown in Fig.7, regardless of the semi-infinite or infinite QD chains, no conductance peak is consistent with any eigenlevel since the molecular states of the QDs become a continuum in such a case. In the case of continuum, although some molecular states decouple from the leads, it can not affect the electron transport for

reasons that the electron transmission paths can not be differentiated. Thus no antiresonance appears in the conductance spectra. However, when investigating the influence of the difference between  $\phi_L$  and  $\phi_R$  on the electron transport, we find that in the situation of  $\phi_L = 0$  and  $\phi_R = 0.5\pi$  the conductance of the infinite QD chain encounters its zero at the down side of energy band, as shown in Fig.7(d). Such a result can be explained as follows. The coupling of a semi-infinite QDs to QD- $l$  indeed brings out the self-energy  $\Sigma_{l\sigma} = \frac{1}{2}(-\varepsilon_0 - i\sqrt{4t_0^2 - \varepsilon_0^2})$ . Then at both sides of the energy band (i.e.,  $\varepsilon_0 = \pm 2t_0$ ), the structure is just transformed into a new double-QD configuration with  $\varepsilon_1 = \varepsilon_2 = \frac{\varepsilon_0}{2} = t_0$ . As a result, in the case of  $\varepsilon_0 = 2t_0$  the bonding state of such a new double-QD structure, which has decoupled from lead-L since  $\phi_L = 0$  and  $\phi_R = 0.5\pi$  (as discussed in the previous paragraph), is aligned with the Fermi level, thereupon, the electron tunneling here presents antiresonance. Alternatively, for the case of  $\phi_L = 0.5\pi$  and  $\phi_R = \pi$  a similar reason gives rise to antiresonance at the position of  $\varepsilon_0 = -2t_0$ . In addition, it is apparent that in the case of  $\phi_L = 0$  and  $\phi_R = \pi$  the conductance is always fixed at zero. This is because that in such a situation any molecular state coupled to lead- $\alpha$  is inevitable to decouple from lead- $\alpha'$ , though the molecular states of the QDs is continuum. Thus, there is still no channel for the electron transport.

#### IV. SUMMARY

With the help of nonequilibrium Green function technique, the electron transport through a QD chain embodied in an AB interferometer has been theoretically investigated. It has been found that for the configurations with the same-numbered QDs coupled to the QDs in the interferometer arms, in the case of  $\phi = 2n\pi$  all odd molecular states of the QDs decouple from the leads, but all even molecular states decouple from the leads when the magnetic flux phase factor is equal to  $(2n - 1)\pi$ . With the increase of magnetic flux from  $(2n - 1)\pi$  to  $2n\pi$ , the antiresonance position in the electron transport spectrum is independent of the change of the decoupled molecular states. By representation transformation, these results are analyzed in detail and the quantum interference in these structures are therefore clarified. When the many-body effect is considered up to the second-order approximation, we showed that the emergence of decoupling gives rise to the apparent destruction of electron-hole symmetry. Finally, the cases of different magnetic fluxes through the two subrings were studied, it showed that via the adjustment of the magnetic flux through either subring, some molecular states would decouple from one lead but still couple to the other, which cause the occurrence of new antiresonances.

At last, we would like to point out that the

theoretical model in the present work can also be regarded as a double-QD AB interferometer with some impurities side-coupled to the QDs in its arms[37, 38], thus the calculated results can mimic

the influence of impurity states on the electronic transport behaviors in such a structure. Therefore, we anticipate that the present work may be helpful for the related experiments.

- 
- [1] J. H. F. Scott-Thomas, S. B. Field, M. A. Kastner, H. I. Smith, and D. A. Antoriadis, *Phys. Rev. Lett.* **62** (1989) 583.
  - [2] U. Meirav, M. A. Kastner, and S. J. Wind, *Phys. Rev. Lett.* **65** (1990) 771.
  - [3] Y. Nagamune, H. Sakaki, P. Kouwenhoven, L. C. Mur, C. J. P. M. Harmans, J. Motohisa, and H. Noge, *Appl. Phys. Lett.* **64** (1994) 2379.
  - [4] Y. Zhang, L. DiCarlo, D. T. McClure, M. Yamamoto, S. Tarucha, C. M. Marcus, M. P. Hanson, and A. C. Gossard, *Phys. Rev. Lett.* **99** (2007) 036603.
  - [5] L. P. Kouwenhoven, N. C. van der Vaar, A. T. Johnson, W. Kool, C. J.P. M. Harmans, J. G. Williamson, A. A. M. Staing, and C. T. Foxon, *Z. Phys. B: Condens. Matter* **85** (1991) 367.
  - [6] D. Goldhaber-Gordon, H. Shtrikman, D. Mahalu, D. Abusch-Magder, U. Meirav, and M. A. Kastner, *Nature (London)* **391** (1998) 156.
  - [7] D. Goldhaber-Gordon, J. Gores, M. A. Kastner, H. Shtrikman, D. Mahalu, and U. Meirav, *Phys. Rev. Lett.* **81** (1998) 5225.
  - [8] S. M. Cronenwett, T. H. Oosterkamp, and L. Kouwenhoven, *Science* **281** (1998) 540.
  - [9] R. J. Heary, J. E. Han, and L. Zhu, *Phys. Rev. B* **77** (2008) 115132.
  - [10] Q. Xie, A. Madhukar, P. Chen, and N. P. Kobayashi, *Phys. Rev. Lett.* **75** (1995) 2542.
  - [11] A. Shailos, C. Prasad, M. Elhassan, R. Akis, D. K. Ferry, J. P. Bird, N. Aoki, L. H. Lin, Y. Ochiai, K. Ishibashi, and Y. Aoyagi, *Phys. Rev. B* **64** (2001) 193302.
  - [12] D. Loss and D. P. DiVincenzo, *Phys. Rev. A* **57** (1998) 120.
  - [13] G. Burkard, D. Loss, and D. P. Divincenzo, *Phys. Rev. B* **59**(1999) 2070.
  - [14] M. Klein, S. Rogge, F. Remacle, and R. D. Levine, *Nano. Lett.* **7** (2007) 2795.
  - [15] W. G. van der Wiel, S. De Franceschi, J. M. Elzerman, T. Fujisawa, S. Tarucha, and L. P. Kouwenhoven, *Rev. Mod. Phys.* **75** (2003) 1.
  - [16] L. W. Yu, K. J. Chen, L. C. Wu, M. Dai, W. Li, and X. F. Huang, *Phys. Rev. B* **71** (2005) 245305.
  - [17] A. Vidan, R. M. Westervelt, M. Stopa, M. Hanson, and A. C. Gossard, *Appl. Phys. Lett.* **85** (2004) 3602.
  - [18] F. R. Waugh, M. J. Berry, D. J. Mar, R. M. Westervelt, K. L. Campman, and A. C. Gossard, *Phys. Rev. Lett.* **75** (1995) 705.
  - [19] I. Amlani, A. O. Orlov, G. Toth, G. H. Bernstein, C. S. Lent, G. L. Snider, *Science* **284** (1999) 289.
  - [20] K. Kobayashi, H. Aikawa, A. Sano, S. Katsumoto, and Y. Iye, *Phys. Rev. B* **70** (2004) 035319.
  - [21] M. Sato, H. Aikawa, K. Kobayashi, S. Katsumoto and Y. Iye, *Phys. Rev. Lett.* **95** (2005) 066801.
  - [22] M. Sigrist, T. Ihn, K. Ensslin, M. Reinwald, and W. Wegscheider, *Phys. Rev. Lett.* **98** (2007) 036805.
  - [23] L. F. Santos and M. I. Dykman, *Phys. Rev. B* **68** (2003) 214410.
  - [24] M. E. Torio, K. Hallberg, S. Flach, A. E. Miroshnichenko, and M. Titov, *Eur. Phys. J. B* **37** (2004) 399.
  - [25] W. Gong, Y. Liu, Y. Zheng, and T. Lü, *Phys. Rev. B* **73** (2006) 245329.
  - [26] B. Kubala and J. König, *Phys. Rev. B* **65** (2002) 245301; D. I. Golosov and Y. Gefen, *Phys. Rev. B* **74** (2006) 205316.
  - [27] P. A. Orellana, F. Domínguez-Adame, I. Gómez, and M. L. Ladrón de Guevara, *Phys. Rev. B* **67** (2003) 085321.
  - [28] H. Lu, R. Lü, and B. F. Zhu, *Phys. Rev. B* **71** (2005) 235320.
  - [29] Q.-F. Sun, J. Wang, and H. Guo, *Phys. Rev. B* **71** (2005) 165310.
  - [30] M. L. Ladrón de Guevara and P. A. Orellana, *Phys. Rev. B* **73** (2006) 205303.
  - [31] K. Bao and Y. Zheng, *Phys. Rev. B*, **73** (2006) 045306.
  - [32] F. R. Waugh, M. J. Berry, D. J. Mar, and R. M. Westervelt, *Phys. Rev. Lett.* **75** (1995) 705.
  - [33] M. Sigrist, T. Ihn, K. Ensslin, M. Reinwald, and W. Wegscheider, *Phys. Rev. Lett.* **98** (2007) 036805.
  - [34] Y. Meir and N. S. Wingreen, *Phys. Rev. Lett.* **68** 2512 (1992);
  - [35] A. P. Jauho, N. S. Wingreen, and Y. Meir, *Phys. Rev. B* **50** (1994) 5528.
  - [36] Y. Liu, Y. Zheng, W. Gong, and T. Lü, *Phys. Lett. A* **360** (2006) 154.
  - [37] Y. Liu, Y. Zheng, W. Gong, and T. Lü, *Phys. Rev. B* **76** (2007) 195326.
  - [38] L. E. F. Foa Torres, H. M. Pastawski, and E. Medina, *Europhys. Lett.* **73** (2006) 170.

FIG. 1: (a) Schematic of the QD chain with two neighboring QDs coupled to both leads. Two magnetic fluxes  $\Phi_L$  and  $\Phi_R$  thread the subrings in the structure. (b) An illustration of the couplings between the molecular states of the QDs and the leads. (c) presents a T-shaped QD structure.

FIG. 2: The linear conductance spectra of N-QD chains with  $N = 2$  to 4. The structure parameters take the values as  $\Gamma = t_m = t_0$ , with  $t_0$  being the unit of energy.

FIG. 3: (a) The conductances of 6-QD system with  $j = 3$ . In (b) The conductances of 8-QD structure are shown in the case of  $j = 4$ .

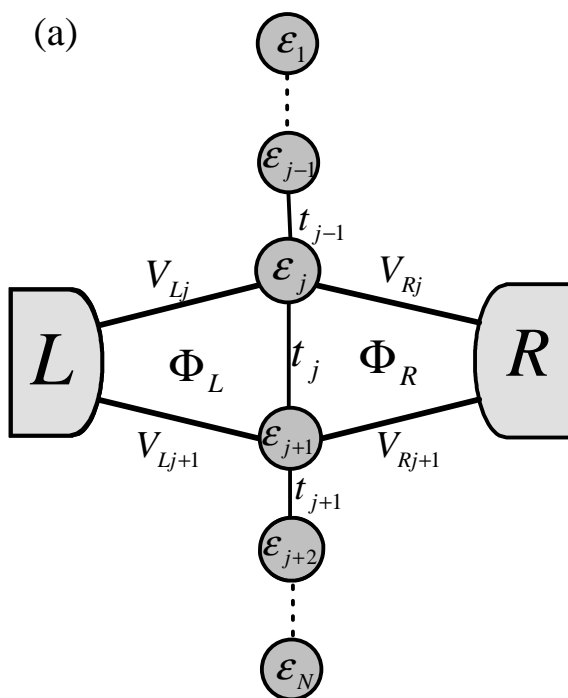
FIG. 4: The linear conductance spectra of double-QD structure with the many-body terms being considered.

FIG. 5: In the presence of many-body terms, the linear conductance spectra of 4-QD structure with  $U = 2t_0$  to  $4t_0$ .

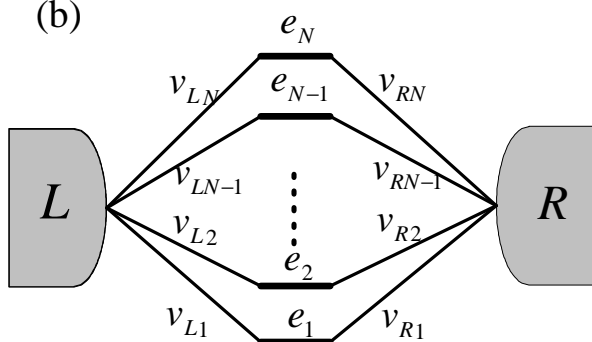
FIG. 6: The calculated conductance spectra of the double-QD and 4-QD structures in the cases of  $\phi_\alpha = n\pi$  and  $\phi_{\alpha'} \neq n\pi$ .

FIG. 7: The conductances of the semi-infinite and infinite QD chains in the absence or presence of magnetic flux.

(a)



(b)



(c)

